ODYSSEV

OPTIMISED DYNAMICS OF HIGH VOLTAGE POWERTRAINS
DEVELOPING SUSTAINABLE SYSTEMS FOR ELECTRIC VEHICLES

D5.1 Motor Topology Optimization Platform Development, first version

KTH

25/07/2026

Funded by
the European Union

Document Information

Issued by:	KTH
Issue date:	25/07/2026
Due date:	30/06/2026
Work package:	WP5
Work package leader:	KTH
Dissemination level:	PU - Public

Document History

Version	Date	Modifications made by
01	10/07/2026	**Meng-Ju Hsieh**
02	17/07/2026	**Montserrat Lanero**
03	24/07/2026	**Luca Peretti**

Authors

First Name	Last Name	Beneficiary
Meng-Ju	Hsieh	KTH
Luca	Peretti	KTH

In case you want any additional information, or you want to consult with the authors of this document, please send your inquiries to: mjhsieh@kth.se

Quality Reviewers

First Name	Last Name	Beneficiary
Antono	Muñoz	CIRCE
Montserrat	Lanero	CIRCE

Disclaimer of Warranties

This document has been prepared by ODYSSEV project partners as an account of work carried out within the framework of the Grant Agreement contract Nº 101192612.

Neither Project Coordinator, nor any signatory party of ODYSSEV Project Consortium Agreement, nor any person acting on behalf of any of them:

- makes any warranty or representation whatsoever, express or implied,
  - with respect to the use of any information, apparatus, method, process, or similar item disclosed in this document, including merchantability and fitness for a particular purpose, or
  - that such use does not infringe on or interfere with privately owned rights, including any party's intellectual property, or
  - that this document is suitable to any particular user's circumstance; or
- assumes responsibility for any damages or other liability whatsoever (including any consequential damages, even if Project Coordinator or any representative of a signatory party of the ODYSSEV Project Consortium Agreement has been advised of the possibility of such damages) resulting from your selection or use of this document or any information, apparatus, method, process, or similar item disclosed in this document.

Executive Summary

The purpose of this deliverable is to establish a technical foundation for the motor development activities by ensuring that topology decisions are aligned with system-level objectives and project requirements. The deliverable provides a common understanding among project partners regarding the selected design direction and the rationale behind key technical decisions.

The audience of this deliverable consists of members of the project consortium, technical work package leaders, and the Project Officer representing the granting authority.

Significant progress has been achieved in consolidating the system-level constraints that will guide the ODYSSEV motor design. The work has identified and translated key powertrain and vehicle-level requirements into an initial set of motor design inputs. In parallel, a Python-based vehicle-level parameter estimation tool has been developed to support the derivation of motor KPIs from demonstrator requirements and representative drive cycles. This constitutes the first software element of the topology-optimization platform and provides a reproducible basis for linking vehicle performance targets with motor sizing. Building on this, the initial framework for a multi-domain topology-optimization algorithm has been defined, where electromagnetic, thermal, mechanical, and sustainability constraints will be progressively integrated to support the selection and refinement of the most suitable high-voltage motor topology for ODYSSEV.

As the project progresses and additional information becomes available from system integration studies, simulations, and validation activities, the topology assessment may be refined. Nevertheless, the present document serves as the baseline reference for subsequent electromagnetic design, optimization, prototyping, and validation activities within the project.

Table of Contents

List of Figures

List of Tables

List of Terms and Definitions

Table 1. Terms and Definitions

Abbreviation	Definition
AC / DC	Alternating Current / Direct Current
AHXS	Adjustable Hybrid X-Switch (Adjustable Hybrid Cross-Switch): The hybrid (Si-IGBT + SiC-MOSFET) inverter topology concept developed in the ODYSSEV project.
Cg / Ct	Turn-to-Ground / Turn-to-Turn Capacitance: Parasitic capacitive elements formed between individual winding conductors, and between conductors and the grounded stator core.
dv/dt	Voltage Gradient: The rate of voltage change over time. High dv/dt transients are typical of fast-switching wide-bandgap inverters and severely stress winding insulation.

E-field	Electric Field: A spatial distribution of electrical force per unit charge. High localized E-field concentrations under high voltage trigger partial discharge.
EESM	Electrically Excited Synchronous Motor: A rare-earth-free machine configuration under evaluation in Task 5.1 that uses a wound rotor field instead of permanent magnets.
EV / BEV	Electric Vehicle / Battery Electric Vehicle
FEA / FEM	Finite Element Analysis / Method: Computerized numerical techniques used to solve complex multi-physics field equations (electrostatic, electromagnetic, thermal).
FOC	Field-Oriented Control: An advanced vector motor control strategy deployed in adjacent work packages (WP4).
GA 101192612	Grant Agreement Number: The unique official identification number under which the EU Horizon Europe ODYSSEV project is funded.
HV	High Voltage: In the context of the ODYSSEV powertrain, this specifically refers to nominal operating voltages spanning the 1200V to 1600V range.
IM	Induction Motor: An asynchronous machine configuration utilizing rotor bars, analyzed within the benchmarking scope (including specialized pole-changing configurations).
iNetic	The industrial partner responsible for establishing chassis housing envelopes and geometric manufacturing limits for the lamination core.
IPMSM	Interior Permanent Magnet Synchronous Motor: The primary baseline machine topology deployed as the unoptimized baseline reference design for the consortium.
MTPA	Maximum Torque Per Ampere: An optimization control strategy designed to minimize stator current magnitude for a given torque requirement.
PD	Partial Discharge: A localized dielectric breakdown of a small portion of a solid or liquid electrical insulation system under high voltage stress.
PDIV	Partial Discharge Inception Voltage: The lowest peak voltage at which partial discharge is first detected within an insulation asset.
PMSM	Permanent Magnet Synchronous Motor: A class of synchronous machines that utilize permanent magnets in the rotor assembly.
PWM	Pulse-Width Modulation: A modulation technique used by the inverter to control the average voltage and current supplied to the electric motor via rapid high-speed switching.
REE	Rare-Earth Element: Heavy permanent magnet elements (such as Neodymium - Nd, Dysprosium - Dy) whose reduction or elimination is prioritized under the project's sustainability constraints.
RWD	Rear-wheel drive
R-road	Tire-road interface, wheel-road friction interface
SiC MOSFET	Silicon Carbide Metal-Oxide-Semiconductor Field-Effect Transistor; a wide-bandgap semiconductor enabling high switching frequencies and low losses.
SSbD	Safe and Sustainable by Design: A strategic product lifecycle framework prioritizing safety, environmental footprint reduction, and hazardous material elimination from early-stage virtual engineering.
UGO	Uncontrolled Generator Operation
WBG	Wide-Bandgap: High-performance semiconductor materials (e.g., SiC) that operate at higher voltages, switching frequencies, and temperatures than conventional silicon.
WP / T	Work Package / Task

1. Introduction

The ODYSSEV project addresses the technological demands of next-generation electric mobility under the Horizon Europe framework. As battery electric vehicles (BEVs) transition toward high-voltage systems operating at 1200V and above, every core element of the traction powertrain must be engineered to withstand increased electrical stresses while delivering superior efficiency. Within this architecture, Work Package 5 (WP5) focuses on the complete virtual synthesis, optimization, and structural development of a highly integrated traction motor system.

This report outlines the initial progress achieved within Task 5.1: "Motor topology development with system constraints" under WP5 of the ODYSSEV project. The primary objective of this task is to develop an advanced, high-voltage, highly efficient traction motor topology capable of operating safely and efficiently under the powertrain's elevated voltage levels (up to 1.2kV in traction mode).

The primary engineering milestones under Task 5.1 are tightly constrained by agreed project Key Performance Indicators (KPIs) to align with Safe and Sustainable by Design (SSbD) directives:

- **Efficiency Map Target:** Achieving an electric machine energy efficiency of at least 95% at the most frequent drive cycle operating points.
- **Material Sustainability:** Fulfilling a strict mandate to achieve a 10% to 20% reduction in heavy rare-earth permanent magnet elements compared to initial design stages.
- **Volumetric Compactness:** Contributing to a combined 3% reduction in overall weight and volume across the coupled converter, machine, and gearbox assembly.

Powertrain Longevity: Optimizing the electromagnetic layout and thermal protection configurations to guarantee a continuous insulation operational lifespan of 150,000 hours under extreme high-voltage switching profiles. To date, the task has successfully established a vehicle-level parameter estimation tool using Python to determine maximum power and torque requirements. Furthermore, a preliminary unoptimized reference motor design based on an Interior Permanent Magnet Synchronous Motor (IPMSM) topology has been developed, fully respecting the geometric and structural envelope constraints provided by industrial partner iNetic. Future activities will focus on broader motor topology benchmarking and advanced cooling method selection to meet the strict Safe and Sustainable by Design (SSbD) principles of the project.

2. Vehicle-Level Performance & Machine KPI Estimation

To derive high-fidelity boundary conditions for the traction motor, a dedicated mathematical script (`calculate_acc_time_Morgan_Plus4.ipynb`) was developed within the KTH open-source electrical machines evaluation workflow.

2.1. Vehicle Baseline Specification: Morgan Plus Four

Morgan Plus Four, was selected as the vehicle demonstrator, as indicated in deliverable 2.6 "ODYSSEV electric powertrain design and blueprint, first version". The parameters for its vehicle dynamic model are assumed and listed in Table 2.

Table 2 Assumed parameters for Morgan Plus Four.

Parameter	Value
Vehicle mass (m_{car}) [kg]	1165
Frontal area (A_f) [m^2]	1.46
Aerodynamic drag coefficient (C_d)	0.55
Rolling resistance coefficient (C_r) of performance tires	0.014
Wheel radius (r_{wheel}) [m]	0.314
Air density (r_{wheel}) [kg/m^3]	1.225
Gear ratio (k_{gear})	10
Efficiency of gearbox (η_{gear}) [%]	97
Friction coefficient: UHP summer tire (μ_{fri})	0.95
Load sensitivity exponent (n_{load})	0.92
Longitudinal distance between the front and rear axles ($l_{wheelbase}$) [m]	2.52
CG height (h_{CG}) [m]	0.35
Fraction of static load on rear axle ($f_{load,rear}$) [%]	55

Target acceleration time, 0-100 km/h [s]	5.2

2.2. Dynamic Force Balance Modelling

2.2.1. Computing Tractive Resistances

At any given instantaneous velocity (v), the script uses a loop to calculate the continuous forces fighting the vehicle's movement:

Aerodynamic Drag: $F_{aero} = \frac{1}{2}\rho_{air} C_d A_f v^2$ (grows quadratically with speed).

Rolling Resistance: $F_{roll} = m_{car} \cdot g \cdot C_r$ (essentially constant).

Grade Resistance: $F_{grade} = m_{car} \cdot g \cdot \sin(\theta)$ (set to 0 if evaluating flat-ground acceleration).

Therefore, total resistance (F_{resist}) is:

$$F_{resist} = F_{aero} + F_{roll} + F_{grade}$$

2.2.2. The Available Tractive Force and Torque Limits

The script evaluates the maximum potential tractive force ($F_{available}$) that can be transmitted from the e-machine to the road. Instead of assuming a generic, static friction coefficient, the tool implements an advanced vehicle dynamics model that dynamically computes the **Traction Limit ($F_{trac,lim}$)** by accounting for **Longitudinal Load Transfer** and **Load-Sensitive Tire Friction Coefficient** at each discrete time step.

Constraint A: The Tire Adhesion/Friction Limit (Low-Speed Threshold)

1. Static Normal Force Assignment ($F_{z,static}$)

First, the base vertical normal force acting on the driven axle under standstill conditions is calculated by

$$F_{z,static} = \frac{m_{car} \cdot g \cdot f_{load,rear}}{n_{drive,axle}}$$

where $f_{load,rear}$ defines the static weight distribution biased toward the driven axle (e.g., rear axle for the *Morgan Plus Four* design architecture), and $n_{drive,axle}$ means the number of drive axles, which is 1 here since *Morgan Plus Four* is rear drive.

2. Dynamic Longitudinal Load Transfer (ΔF_z)

When the vehicle undergoes acceleration, inertial forces cause a dynamic shift of vertical load from the front axle to the rear axle. The script updates this dynamic change using the acceleration from the previous time step (a_{prev}) by

$$\Delta F_z = \frac{m_{car} \cdot a_{prev} \cdot h_{CG}}{l_{wheelbase}}$$

where h_{CG} represents the center of gravity height and wheelbase represents the longitudinal distance between the front and rear axles. For a rear-wheel-drive (RWD) vehicle like the Morgan Plus Four, this adds vertical force to the rear wheels ($F_z = F_{z,static} + \Delta F_z$), significantly boosting the available traction during intense wide-open-throttle (WOT) launch conditions.

3. WOT/Load-Sensitive Friction Coefficient (μ_{eff})

Tire rubber exhibits non-linear behavior where the effective friction coefficient degrades as the vertical load increases (known as tire load sensitivity). The script models this phenomenon using a sensitivity exponent (n_{load}) by

$$\mu_{eff} = \mu_{ref} \cdot \left(\frac{F_z}{F_{z,static}}\right)^{n_{load}-1}$$

where μ_{ref} is the nominal friction coefficient under static load. This formulation ensures that the framework captures the true physical limits of tire-road contact mechanics under high-torque transient states.

4. Ultimate Traction Boundary ($F_{trac,lim}$)

Finally, the maximum boundary force physically transmitted by the tires without spinning is formulated as:

$$F_{trac,lim} = \mu_{eff} \cdot F_z \cdot n_{drive,axle}$$

Constraint B: The Motor Electromagnetic Profile (The Torque-Speed Envelope)

As the vehicle speed increases, the limits shift from the tires to the electric machine itself. The script models a classic traction motor curve split into two zones:

Constant Torque Region (Below Base Speed n_{base}): The motor delivers its absolute maximum peak torque ($T_{em,max}$). The tractive force at the wheels is flat

$$F_{em,max} = \frac{T_{em,max} \cdot k_{gear} \cdot \eta_{gear}}{r_{wheel}}$$

where k_{gear} is the gear ratio and η_{gear} is the efficiency of the gearbox.

The script applies a min() function boundary to choose the true available acceleration force at any instant:

$$F_{available} = \min(F_{trac,lim}, F_{em,max})$$

2.2.3. Numerical Integration (Kinematics)

Once the actual accelerating force is known ($F_{acc} = F_{available} - F_{resist}$), Newton's second law computes the instantaneous acceleration:

$$a = \frac{F_{acc}}{m_{car} \cdot (1 + \epsilon)}$$

where $\epsilon = 0.006$ *is a guess parameter for the rotational inertia factor of the spinning wheels, shafts, and rotor [1].*

Using small discrete time steps (Δt, e.g., 0.01 seconds), the script updates the state variables iteratively:

New Velocity: $v_{new} = v_{old} + a \cdot \Delta t$

New Distance: $x_{new} = x_{old} + v_{old} \cdot \Delta t$

The loop breaks the exact moment v_{new} reaches 100 km/h (27.78 m/s), and outputs the total elapsed time.

2.2.4. Drive Cycle Selection Strategy for Multi-Regional Sizing Robustness

To extract highly representative efficiency maps and prevent over-fitting the machine optimization to a singular regional test profile, the vehicle evaluation notebook incorporates a comprehensive multi-cycle diagnostic dictionary. These selections allow the framework to capture a diverse spectrum of speed distributions, stop-and-go patterns, acceleration gradients, and steady-state cruise states across major international standard configurations and transient real-world cycles. Future optimization work and KPI extraction may use one of the following profile – a decision will be taken after closer discussions with Morgan representatives, who should be able to give us a better indication of which profile is more representative for the Plus Four typical drive cycle.

1. Global Regulatory Standards (WLTC, JC08, FTP72/UDDS, HWFET)

WLTC Cl.3 (WLTC Class 3): The primary reference for European compliance. It represents the standard for high-power-to-weight vehicles with varying dynamics, covering urban, suburban, rural, and highway operations.

jpjc08 (JC08): Represents highly congested Japanese urban contexts characterized by frequent idling periods, lower average speeds, and soft, repeated acceleration phases.

FTP72UDDS (FTP-72 / Urban Dynamometer Driving Schedule): The foundational US EPA urban drive test representing traditional heavy city stop-and-go behaviour.

HWFET (Highway Fuel Economy Test): A steady-state US EPA highway cruising cycle used to map high-speed continuous motor operational efficiency and flux-weakening boundary iron losses.

2. High-Load and Aggressive Operational Profiles (US06, UCLA92)

US06 (Supplemental FTP): A high-acceleration, aggressive US cycle designed to capture driving behaviors omitted by classical tests. It forces the simulation loop to capture high peak motor current and extreme mechanical/thermal transient stress points.

UCLA92 (Unified Cycle): A sharper, higher-speed urban/suburban alternative to the standard UDDS cycle, incorporating higher maximum speeds and acceleration rates.

3. Real-World Transient Micro-Trips (CADC / Artemis Suite)

To reflect physical on-road behaviour beyond artificial laboratory step-traces, the **Common Artemis Driving Cycles (CADC)** are utilized:

Artemis URBAN: Captures chaotic city traffic with high transient speed fluctuations.

Artemis RURAL: Simulates typical European inter-city secondary routes.

Artemis MW.130 (Artemis Motorway 130): An aggressive high-speed highway test peaking at 130 km/h, isolating aerodynamic load overcoming limits and long-term continuous thermal performance targets.

4. Hyper-Congested Stop-and-Go Bounds (NYCC)

NYCC (New York City Cycle): An extreme low-speed urban cycle with low average velocities and high frequency of idle time. This boundary condition maps the low-speed copper loss boundaries and thermal hot spots generated by stator resistance during prolonged low-speed maximum torque demand.

2.3. Simulation Results & Target Motor KPIs Extraction

The vehicle kinematics framework maps the discrete time-series data from the comprehensive drive cycle database onto the physical limits of the vehicle demonstrator. The relationships between linear velocity, time profiles, and the resulting electromagnetic and power electronic boundaries are evaluated via Figures 1 through 5.

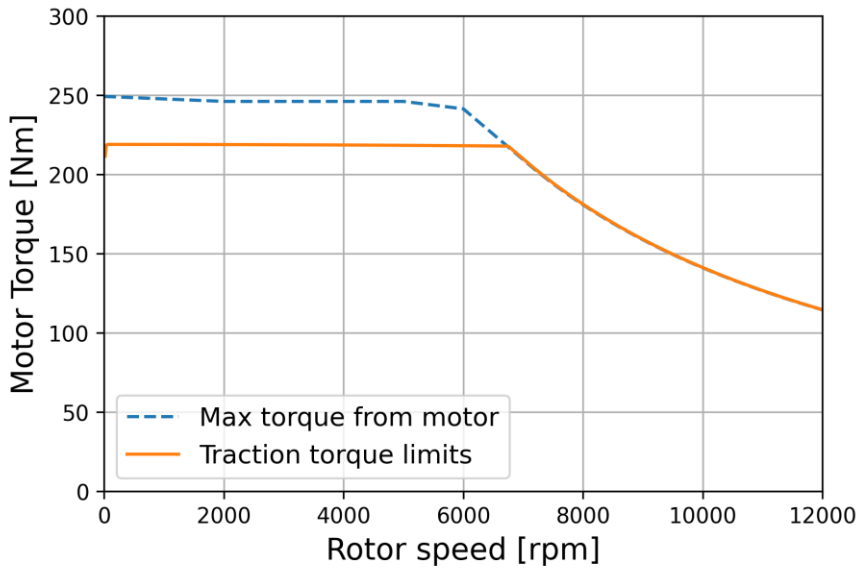

Figure 1: Motor torque vs. speed.

Figures 1 and 2 illustrate the torque-speed operational limits at the motor shaft and wheel hub sides, respectively. In these plots, the dashed profiles represent the absolute peak electromagnetic torque capability of the motor, while the solid lines incorporate the dynamic traction friction limit under longitudinal load transfer.

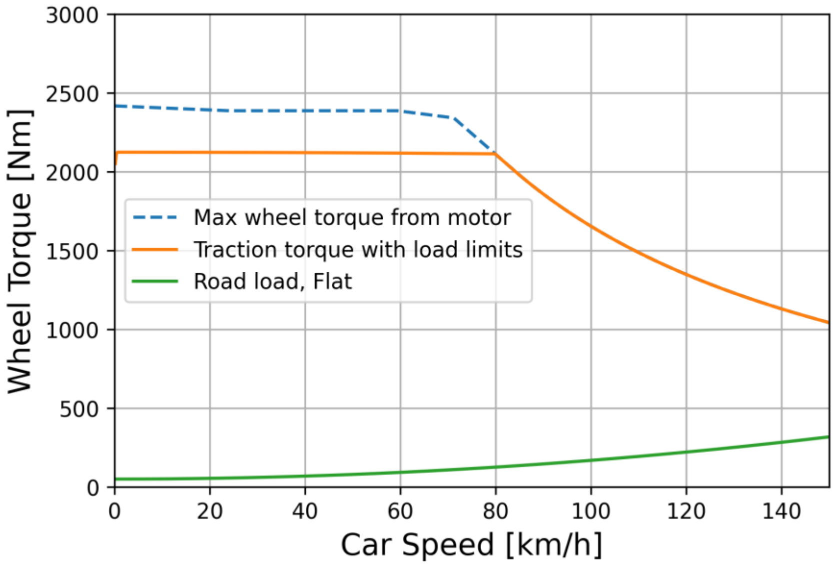

Figure 2 Wheel torque and road load vs. car speed.

Driven by the mechanical gear ratio, the wheel traction torque scales to approximately ten times the motor shaft torque. The constant-torque region of the motor saturates at 220–230 Nm, maintaining this plateau until intersecting the corner base speed boundary at 6,500–7,000 rpm, where field-weakening initiates. Furthermore, the time-domain velocity trace shown in Figure 3 confirms that the selected maximum torque envelope satisfies the dynamic performance requirements of the Morgan Plus Four demonstrator, successfully achieving the 0–100 km/h sprint target in 5.2 seconds.

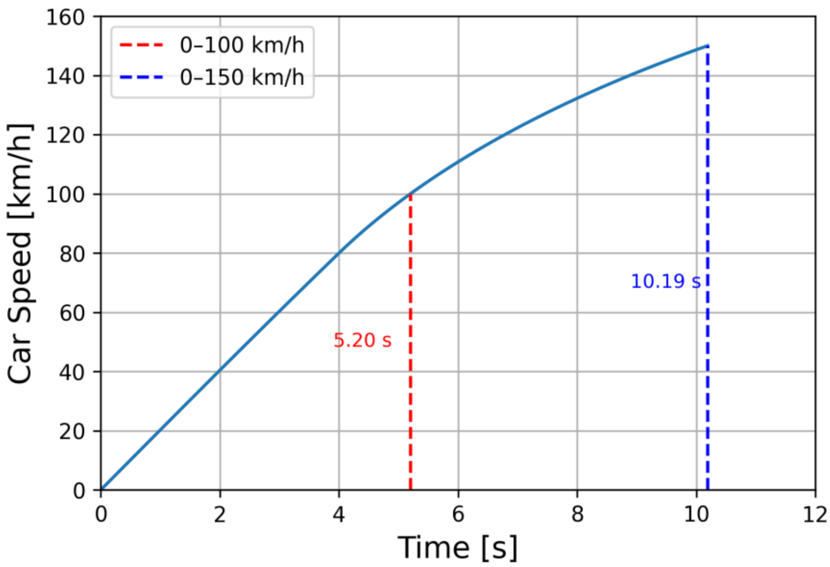

Figure 3 Acceleration profile.

To evaluate the required power level and structural boundaries of the machine, Figures 4 and 5 overlay the operational scatter points from the extensive drive cycle diagnostic dictionary directly against the peak vehicle boundaries. The numerical simulation demonstrates that the motor successfully encloses all multi-regional driving cycles. High-transient performance profiles, most notably the US06 and Artemis URBAN cycles, cluster tightly along the low-speed maximum torque envelope, justifying the specified peak saturation limits.

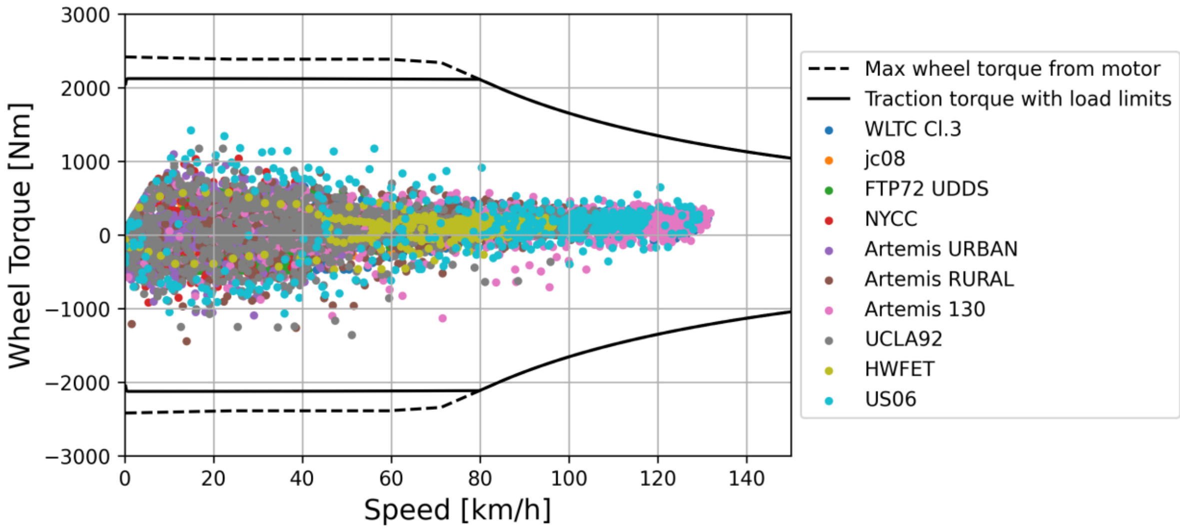

Figure 4 Wheel torque vs. car speed and operating points from selective drive cycles.

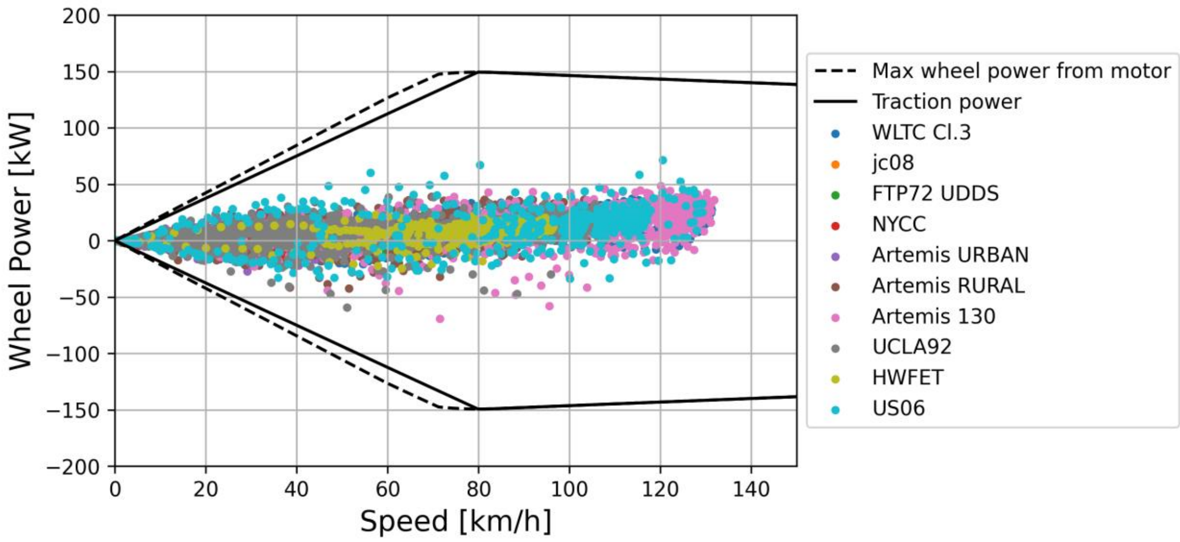

Figure 5 Wheel power vs. car speed and operating points from selective drive cycles.

Based on these consolidated kinematics and drive cycle mapping results, the preliminary target key performance indicators (KPIs) for the ODYSSEV traction motor topology optimization loop have been established in Table 3.

Table 3 Preliminary Traction Motor Target KPIs (Demonstrator Sizing Loop).

Parameter	Target	Engineering Rationale
Peak Torque	220 – 240 Nm	Constrained by dynamic RWD R-road friction boundary
Base Speed	6,500 rpm	Corner frequency for high-voltage inverter switching transition
Peak Power	150 kW	Required for dynamic 0–100 km/h performance target (5.2s)
Continuous Power	100 kW	Maximum continuous load envelope during high-speed cruise

3. Motor Design: From Rating to Sizing

With the macroscopic vehicle-level performance ratings and preliminary target motor KPIs established in Table 3. Task 5.1 transitions into mapping these requirements into explicit physical boundaries. As illustrated in the development workflow, the numerical ratings act as initial inputs to analytical core sizing laws. However, moving from an unoptimized analytical baseline to a finalized traction motor design requires the simultaneous integration of four multi-physics engineering domains, necessitating careful balancing and multi-objective design trade-offs:

1. Electromagnetic
    a. Torque & power targets
    b. Motor topology
    c. Voltage & current level
    d. Power factor

   e. Losses
2. Thermal
   a. Cooling pump power
   b. Coolant type
   c. Flow rate
   d. Pressure drop limit
   e. Inlet/outlet temperatures
   f. Single/dual cooling circuits
3. Mechanical
   a. Structural integrity
   b. Packaging constraints
   c. Vibration & NVH performance
   d. Manufacturing feasibility
   e. Assembly & sealing
4. Sustainability
   a. Heavy rare-earth material usage
   b. Raw material circularity & choice of secondary elements
   c. Operational energy efficiency

The following updates of this deliverable, D5.5 (December 2026) and D5.6 (June 2027), will consider how each domain is translated into optimization constraints or objective functions.

3.1. Motor Topology Selection

3.1.1. Conventional Motor Topology Review

Conventional and advanced configurations under review within the Task 5.1 design matrix include standard Permanent Magnet Synchronous Motors (PMSMs), Permanent Magnet Assisted Synchronous Reluctance Motors (PMaSynRMs), traditional Induction Motors (IMs), and Electrically Excited Synchronous Motors (EESMs). The main difference between these motor topologies lies in how they produce the rotor magnetic field and, in turn, how they generate electromagnetic torque.

1. **PMSMs**
   The PMSM configuration generates its rotor magnetic field through high-energy permanent magnets embedded deep within the rotor lamination stacks. Torque production is a hybrid combination of magnetic alignment torque and reluctance torque caused by rotor saliency ($L_q > L_d$). This topology provides exceptional low-speed torque density and peak power capacity. However, under high-voltage 1200V operation, the constant presence of the magnet flux induces significant iron core losses during high-speed field-weakening regimes. Furthermore, its reliance on heavy rare-earth elements conflicts with the project's target to reduce critical raw materials by 10% to 20%.
2. **PMaSynRMs**
   The PMaSynRM relies primarily on reluctance torque, which is maximized by shaping highly engineered, high-saliency rotor flux barriers that guide the magnetic flux along low-reluctance paths (d-axis). To boost the power factor and torque density without heavily relying on critical minerals, a minimal volume of low-cost or non-heavy rare-earth permanent magnets is inserted into the flux barriers to counteract the stator's leakage flux. This hybrid approach significantly reduces total rare-earth mass compared to a traditional PMSM, lowering manufacturing costs and environmental impacts. The structural trade-off

requires optimizing the intricate lamination bridges to withstand centrifugal stresses at high speeds while preventing magnetic flux leakage from bypassing the active air gap.

3. **IMs**
   Induction Motors establish their rotor magnetic field via electromagnetic induction, where stator-fed currents induce alternating voltages across a short-circuited rotor cage assembly. Because torque is generated entirely through the slip-frequency interaction between the rotating stator field and the induced rotor currents, the machine eliminates the need for permanent magnets, thereby bypassing critical raw-material dependence. Mechanically robust and naturally fault-tolerant, the IM eliminates the risk of high-speed UGO because the rotor field decays immediately upon stator de-energization. However, the continuous current flow through the rotor cage yields persistent rotor copper losses, which inherently lower part-load efficiency and challenge the project's mandate of achieving a 95% efficiency target at the most frequent drive cycle operating points.
4. **EESMs**
   EESMs replace permanent magnets with a dedicated wound-field rotor fed by an external DC excitation source via slip rings or brushless inductive exciters. Torque is produced by the alignment of the stator field with this actively controlled rotor field. The primary advantage of the EESM is its flexibility in control; the rotor field can be dynamically tuned to optimize efficiency across all part-load regions, and it can be completely de-energized during high-speed highway cruising to eliminate iron losses and UGO risks. The engineering trade-off for this topology involves increased mechanical complexity, brush wear considerations (if slip rings are used), and additional copper losses within the rotor windings that must be mitigated by the thermal cooling system.

3.1.2. Novel Motor Topology Alternatives

1. **Pole-Changing IM (PCIM)**
   The PCIM topology modifies the traditional IM blueprint by introducing a reconfigurable stator winding layout capable of altering the active magnetic pole count during operation. By electronically changing the winding connections via the high-voltage inverter switching matrix, the machine can switch between a high-pole configuration for high-torque, low-speed launch conditions (such as the initial wide-open-throttle acceleration of the Morgan Plus Four) and a low-pole configuration for high-speed motorway cruising. This capability drastically broadens the efficient operating speed range without requiring a mechanical multi-speed gearbox, supporting the project target of a 1-3% overall powertrain volumetric and weight reduction. Furthermore, because it retains a robust rotor cage structure, it completely eliminates the reliance on heavy rare-earth elements, aligning with the project's sustainability directive. The engineering trade-off for this topology involves the significant increase in stator slot insulation stresses and control complexity required to manage transient current spikes during the pole-switching phase under 1200V excitation.
2. **Asymmetric IPMSM**
   The Asymmetric IPMSM alters the classical symmetrical arrangement of rotor permanent magnets and flux barriers by implementing an intentional geometric asymmetry across adjacent rotor poles or pole halves. In a standard IPMSM, multi-layer V-shape or delta-shape magnet barriers are identical, which can lead to concentrated magnetic saturation and high torque ripple. By rendering the flux barriers asymmetric, the optimization framework can intentionally phase-shift the spatial harmonics of the air-gap magnetic flux density. This design layout significantly minimizes torque ripple and suppresses Acoustic Noise, Vibration, and Harshness (NVH) profiles across the wide operational speed range. Additionally, this asymmetry can be optimized to enhance the reluctance torque component selectively in the motoring quadrant, allowing the machine to satisfy the peak performance torque boundary (220–250 Nm) using a reduced permanent magnet mass. This directly contributes to the project mandate of achieving a 10-20% reduction in critical raw materials while maintaining a high power factor.
3. **Harmonic-Harvesting EESM**

The Harmonic-harvesting EESM represents a major evolution over conventional wound-rotor synchronous machines by eliminating the reliability vulnerabilities associated with mechanical slip rings or separate bulky brushless exciters. This novel topology utilizes specialized stator winding arrangements or inverter switching strategies to deliberately inject a specific spatial or temporal time-harmonic (typically the 3rd harmonic) into the air-gap magnetic field. The rotor is equipped with an auxiliary winding connected to an onboard rectifier bridge that is tuned to intercept and capture this specific harmonic energy, converting it directly into the DC excitation current required by the main rotor field coils. By utilizing these inherent air-gap field harmonics, the EESM gains brushless self-excitation capabilities. This topology provides an exceptionally flexible efficiency map because the rotor field can be actively optimized or completely de-energized during high-speed highway cruise cycles to eliminate iron core losses and remove UGO voltage clamping risks. The design trade-off centers on highly complex multi-layer winding layouts and specialized finite element verification to balance core saturation limits against harmonic harvesting efficiency.

The selection of a conventional or a novel motor topology for this project is subjected to the fulfillment of the declared motor KPIs, and is subjected to the analysis of and optimization of such topologies for the specific vehicle case. This activity is the core work that will be conducted and continuously reported in the next deliverables.

3.2. Cooling Strategy and Thermal Management Integration

Operating under the 1200V powertrain architecture with strict limits on continuous power density requires an advanced thermal management framework to maintain motor performance and prevent winding insulation failure over the targeted 150,000-hour system lifespan. While conventional housing water jackets serve as a standard industrial baseline, they introduce a high conductive thermal resistance between the heat-generating copper slots and the external coolant loop. Heat must travel through the slot liners, the stator lamination core, and the housing mechanical interfaces before being dissipated by the fluid stream. This extended thermal path results in steep temperature gradients and localized hotspots during aggressive transient cycles (such as the US06 profile). To maximize thermal dissipation, lower thermal resistance, and successfully achieve the 100 kW continuous power requirement derived from the vehicle sizing loop, the following advanced cooling strategies will be explored in WP5:

1. **Hollow-Shaft Rotor Cooling**
   Hollow-shaft rotor cooling targets the primary heat sources within the rotating assembly, which is particularly critical for preventing permanent magnet demagnetization in IPMSM/PMaSynRM topologies or mitigating copper losses in wound-rotor EESM configurations. This strategy utilizes a central fluid conduit machined directly inside the rotor shaft, through which a dielectric oil or dedicated coolant is pumped. As the fluid flows axially through the spinning shaft, heat is transferred away from the rotor core via forced convection.
   The primary advantage of this topology is its excellent continuous high-speed thermal regulation, which directly counters the rotor iron core losses generated during deep field-weakening regimes. However, this method introduces significant engineering trade-offs, including the need for specialized high-speed rotational seals to prevent fluid leakage into the air gap, precise fluid channel positioning to avoid disrupting the mechanical rotor dynamic balance, and additional pump power to overcome centrifugal pressure drops.
2. **In-Slot Winding Cooling**

In-slot winding cooling directly tackles the primary thermal bottleneck of the machine by embedding micro-channel cooling tubes, cold plates, or dedicated dielectric fluid conduits inside the stator slots alongside the active copper conductors. By bringing the cooling medium into immediate proximity with the primary heat source, this strategy bypasses the thermal resistance of the stator iron teeth and yoke entirely, maximizing the continuous current density capacity of the machine. This configuration is highly effective for suppressing the significant copper losses encountered during low-speed high-torque launches. Nevertheless, implementing in-slot cooling channels within a high-voltage 1200V winding structure raises serious manufacturing feasibility challenges. The presence of cooling channels inevitably reduces the net copper slot fill factor, complicates the insulation wrap assembly, and requires absolute sealing integrity to eliminate the risk of coolant leakage under continuous operating vibrations, which would lead to immediate catastrophic dielectric breakdown.

3. **End-Winding Cooling**
   End-winding cooling addresses the localized hotspots that naturally develop at the axial extensions of the stator windings, where the copper turns lack the structural heat sinking provided by the iron lamination stack. This strategy is primarily executed via direct oil spray cooling, where dedicated nozzle manifolds project a low-viscosity dielectric oil onto the exposed end-windings, or through localized encapsulation methods using high-thermal-conductivity potting resins coupled to housing heat exchangers.
   Direct fluid-wetting provides exceptional heat transfer coefficients, accelerating thermal drawdown during high peak power acceleration states. The main trade-offs associated with aggressive end-winding oil spray loops center on fluid management complexity; the design must precisely balance the fluid flow rate and nozzle pressure drop limits to maximize thermal performance while simultaneously minimizing windage losses caused by the rotor spinning against the surrounding fluid mist, ensuring overall powertrain efficiency is maintained.

Different cooling solutions will allow different current density values in the windings, thus affecting the physical size of the propulsion system given the torque and power requirements. An overall evaluation that balances the best cooling system solution for the motor, its cost, its reliability, and its integration with the rest of the cooling system for the batteries and the converters is going to be part of the activities in WP2.

3.2.1. Direct Oil Jet and Spray Cooling

Within the strategies outlined above, the highest heat transfer performance is offered by direct oil cooling, in which a dielectric oil is brought into contact with the winding surfaces either as impinging jets or as an atomized spray. Because the coolant wets the conductors directly, the conductive path through slot liner, lamination stack, and housing is bypassed, and heat transfer coefficients of several thousand W/m^2K become achievable, well above the effective slot to coolant conductance of a conventional housing water jacket. Jets concentrate a very high coefficient in a small stagnation region and suit targeted hot spots, while sprays distribute a lower peak coefficient over a wider area of the end windings. The practical limit is set by fluid management: nozzle pressure drop, pump power, oil temperature rise, and windage losses must be balanced against the thermal gain. UCL leads this activity and provides the measured cooling constraints that enter the WP5 design optimization and the WP2 thermal integration.

To place the cooling design on a measured basis rather than on literature correlations, UCL has commissioned a single jet impingement rig at its Advanced Propulsion Laboratory, shown schematically in Figure 6. Oil is pumped through a flow meter and an instrumented lance, whose pressure drop is recorded, and jets onto the top face of a heated copper cylinder. Four in line thermocouples spaced 15 mm apart resolve the axial temperature gradient, from which the heat flux is obtained by Fourier's law and the surface temperature by extrapolation, with radial losses estimated and subtracted. The heat transfer coefficient is then evaluated as $h = \dot{q}/(T_s - T_{in})$, with the oil inlet temperature measured immediately upstream of the nozzle. The same measurement chain is mirrored in an in house interactive thermal design tool, so that measured coefficients can be applied directly to candidate winding geometries.

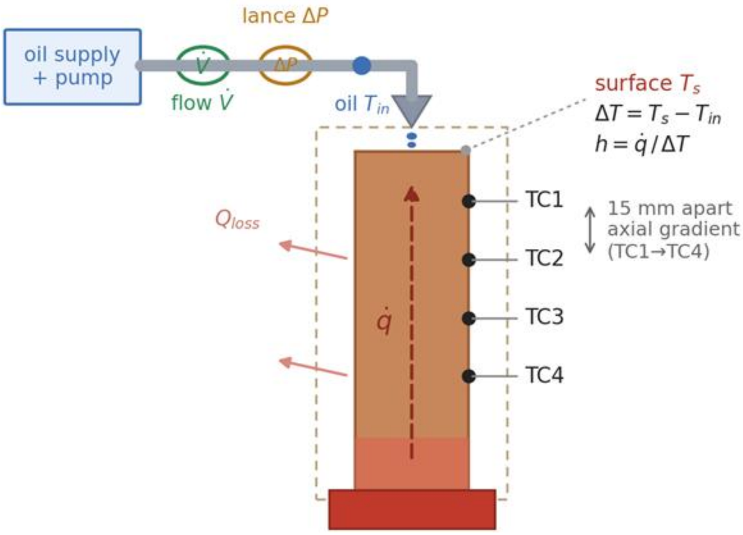

Figure 6 Single jet oil impingement rig at UCL for direct measurement of the heat transfer coefficient

Figure 7 summarizes the first measurement campaign, covering three nozzle geometries over oil flow rates from 0.04 to 0.86 L/min per nozzle. The heat transfer coefficient rises steadily with flow, from about 700 W/m^2K at the lowest flow to roughly 2,500 to 2,900 W/m^2K at 0.3 to 0.4 L/min for the M5 nozzles, and reaching about 6,500 W/m^2K at 0.86 L/min with the 1.0 mm stainless steel nozzle. These are single jet values on a flat copper target; at machine level they scale with the number of nozzles in the manifold. The data are preliminary, and the influence of oil temperature, and hence viscosity, standoff distance, and surface orientation remains to be characterized.

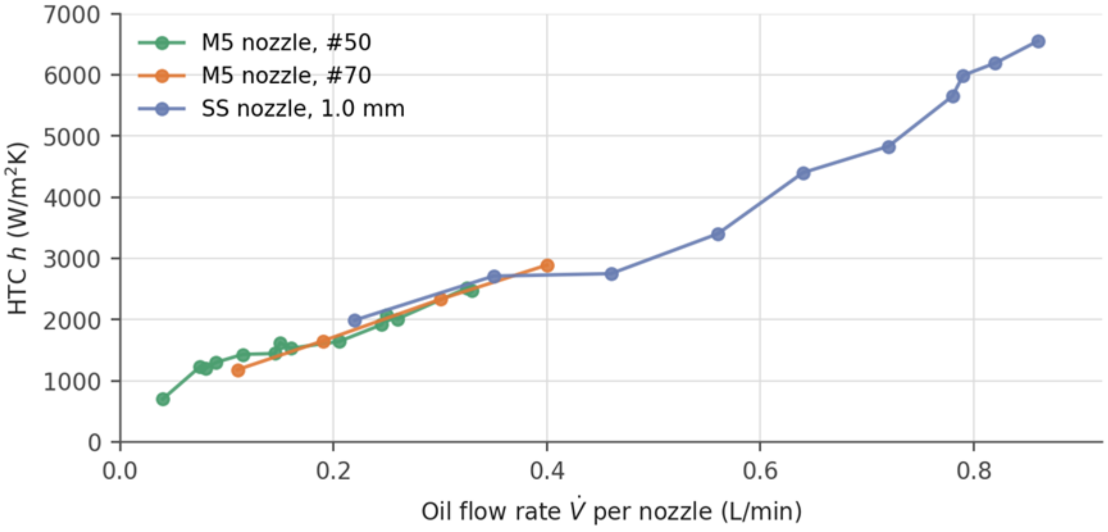

Figure 7 Measured heat transfer coefficient versus oil flow rate for three nozzle geometries (single jet, flat copper target).

The planned workflow is measure first, then design. The characterization will be completed across nozzle type (plain orifice jets and atomizing spray nozzles), nozzle diameter, flow rate, standoff distance, and oil inlet temperature, and condensed into nondimensional correlations suitable for the machine thermal network model. These correlations will then be used to size the nozzle count, placement, and total oil flow for the end winding and slot regions of the reference machine, so that the selected cooling architecture and the admissible winding current density in the WP5 optimization loop rest on measured data. The resulting flow and pressure budgets, together with the oil temperature rise, will be passed to WP2 for integration with the battery and converter cooling circuits.

3.3. Reference Motor Design: Initial IPMSM Topology

To allow overlapping work packages (such as WP4 for the 3-level AHXS inverter development and WP2 for structural thermal packaging) to advance without waiting for the full execution of the optimization loop, a preliminary baseline design has been completed.

- Topology Choice: IPMSM using embedded V-shape internal permanent magnets to achieve high torque density and extensive field-weakening flexibility.
- Geometric Limits: The active stack length, shaft constraints, and stator outer diameter boundaries of the largest commercial motor solution provided by industrial partner iNetic were used as hard geometric limits [2].Current Status: This initial reference design satisfies the unoptimized baseline requirements of the Morgan Plus Four vehicle profile and fits within iNetic's structural boundaries [2].

In Figure 6 and Table 4 are the performance of the initial design, which will be further expanded with more details and parameters as the optimization process continues in following versions (D5.5 and D5.6). It can be observed that under ideal full-voltage utilization conditions, the initial benchmark design satisfies the baseline vehicle acceleration mandates. However, when accounting for realistic system-level limitations, such as the non-ideal voltage drops across the wide-bandgap inverter switches, safety margins, and transient impedance restrictions, the effective voltage available to the motor terminals is reduced, causing the vehicle performance to fall short of the target demand. This critical discrepancy highlights the vital importance of considering system-level voltage margins and high-frequency parasitic parameters early in the multi-physics optimization loop, rather than relying solely on idealized ideal-source simulations.

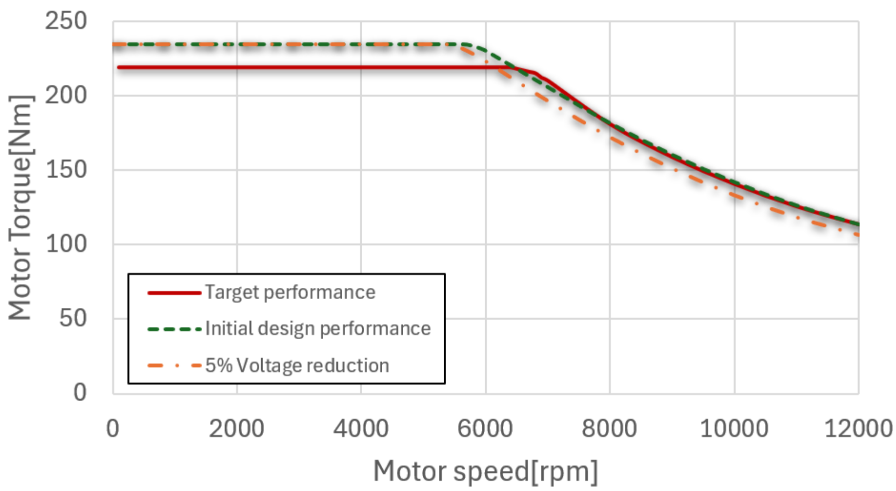

Figure 8 Maximum torque envelopes for target one and initial design with full and 95% voltage utilization

Table 4 Motor KPIs for initial design.

Parameters	Value
DC link Voltage [V]	1200
Peak power [kW] (10s)	150
Continuous power [kW]	100
Max. Torque [Nm]	230
Max. RMS Current [A]	150
Weight [kg]	50

4. Conclusions

This report summarizes the foundational milestones successfully achieved under Task 5.1: "Motor topology development with system constraints" within WP5. By adopting a rigorous, top-down engineering methodology, the project has successfully bridged high-level vehicle performance parameters with explicit electromagnetic design boundaries. The development and deployment of the KTH vehicle kinematics and requirement mapping tool have provided a scientifically sound empirical baseline. By dynamically incorporating advanced chassis physics—specifically longitudinal load transfer and load-sensitive non-linear tire friction behaviors, the tool successfully translated the aggressive 5.2-second 0–100 km/h acceleration mandate of the Morgan Plus Four reference sportscar into a concrete traction motor specification envelope. The initial core sizing bounds are now definitively set, establishing a target peak power of 150 kW, a continuous cruising threshold of 100 kW, a maximum saturation torque of 220–240 Nm, and a corner base speed of approximately 6,500 rpm.

Simultaneously, the collaborative structural integration has been safeguarded against multi-partner development delays by delivering an initial, unoptimized Interior Permanent Magnet Synchronous Motor (IPMSM) reference layout. Adhering to the non-negotiable housing envelope constraints provided by iNetic, this 48-slot, 8-pole benchmark design validated the derived maximum shaft torque target by yielding 230 Nm under 1200V system constraints. This reference model has already been successfully disseminated across the consortium during WP technical meetings and monitoring meetings (Steering Committee), enabling adjacent work packages to proceed with structural thermal integration modelling in WP2 and inverter control loop tuning (such as FOC and MTPA strategies) in WP4.

The next steps include further discussions with iNetic and Morgan to familiarize with more detailed technical data on the Plus Four, which will be used to optimize the motor design, as well as the investigation of a design with less (or no) magnets at all, compared to the initial IPM design presented in this report.

5. References

[1] T. D. Gillespie, Fundamentals of Vehicle Dynamics, SAE International, 1992, available: https://ieeexplore.ieee.org/book/8854937

[2] iNetic Traction, “Powering Performance: Precision Motor and Inverter Pairing for Automotive Excellence”, available: https://inetictraction.com/wp-content/uploads/2025/09/rEV-5U-WN025.pdf

ODYSSEV

GA 101192612

PARTNERS

FOLLOW US

Funded by the European Union under GA no. 101192612. Views and opinions expressed are however those of the author(s) only and do not necessarily reflect those of the European Union or CINEA. Neither the European Union nor the granting authority can be held responsible for them.

Funded by the European Union